

In Situ XANES of an Iron Porphyrin Irreversibly Adsorbed on an Electrode Surface

Sunghyun Kim,[†] In Tae Bae,[‡] Marnita Sandifer,[†] Philip N. Ross,[§] Roger Carr,[⊥] Joseph Woicik,[‡] Mark R. Antonio,[‡] and Daniel A. Scherson^{*†}

Contribution from the Case Center for Electrochemical Sciences and the Department of Chemistry, Case Western Reserve University, Cleveland, Ohio 44106, BP Research, 4440 Warrensville Center Road, Cleveland, Ohio 44128-2837, Lawrence Berkeley Laboratory, 1 Cyclotron Road, Berkeley, California 94720, Stanford Synchrotron Radiation Laboratory, Stanford, California 94305, and National Institute of Standards and Technology, Gaithersburg, Maryland 20899. Received January 23, 1991

Abstract: In situ iron K-edge X-ray absorption near edge structure, XANES, has been employed to examine the axial coordination of (μ -oxo)bis[iron *meso*-tetrakis(4-methoxyphenyl)porphyrin] (FeTMPP)₂O, irreversibly adsorbed on a high area carbon substrate, Black Pearl (BP), as a function of applied potential. Analysis of the XANES provides conclusive evidence that the coordination about Fe^{3+} in the supported, fully oxidized macrocycle is remarkably different from that about Fe^{2+} in the corresponding fully reduced macrocycle. In the adsorbed, oxidized state, (FeTMPP)₂O retains its μ -oxo character and it undergoes a two-electron reduction to yield predominantly four-coordinate square-planar FeTMPP without axial ligation.

Introduction

The adsorption of a variety of atomic and molecular species on electrode surfaces has been found to promote the rates of a growing number of electron-transfer processes of fundamental and technological importance.¹ Essential to the further elucidation of the factors underlying this phenomenon is a better understanding of the changes in the electronic and structural characteristics of these species induced by the binding to the surface and by variation in the externally applied potential.

The rather recent advent of synchrotron radiation has opened new prospects for the development and implementation of in situ methods with which some of these changes can be probed.² Although remarkable success has been achieved in in situ studies involving atomic adsorption on single-crystal substrates,³ applications of these techniques to the in situ study of molecules adsorbed at monolayer coverages on electrode surfaces have been very limited.⁴ This may be attributed, in part, to the relatively small number of molecules that can be accommodated on a nominally smooth surface even at saturation coverages (ca. 10^{-10} – 10^{-11} mol·cm⁻²), a factor that makes detection exceedingly difficult. Low-Z, high area supports, such as carbon, afford a convenient means of increasing the number of molecules exposed to the X-ray beam without introducing large losses due to radiation attenuation. In fact, this strategy has been used with much success in in situ studies involving ⁵⁷Fe Mossbauer-effect spectroscopy.⁵ Besides its relative transparency to high-energy radiation and high electronic conductivity, the advantages of carbon over other kinds of supports are 2-fold: it displays high affinity for certain molecular species, a property associated in part with the presence of surface functional groups, and it exhibits little or no activity for many electrochemical processes of interest.

This paper presents in situ iron K-edge X-ray absorption near edge structure, XANES, spectra for (μ -oxo)bis[iron *meso*-tetrakis(4-methoxyphenyl)porphyrin], (FeTMPP)₂O, irreversibly adsorbed on Black Pearl (BP), a high area carbon with about 1000 m²·g⁻¹, in aqueous electrolytes. Some of the properties of this specific adsorbate–substrate system have been investigated with in situ ⁵⁷Fe Mossbauer-effect spectroscopy.⁵ The information derived from the Fe XANES experiments described herein complements the previous Mossbauer results and, most importantly, provides conclusive evidence regarding the modifications in axial coordination and oxidation state of iron associated with the surface-bound redox process.

Experimental Section

(FeTMPP)₂O was synthesized and purified according to procedures specified in detail elsewhere.⁶ Tetracoordinated, square-planar iron(2+) phthalocyanine (FePc) was obtained from Eastman Kodak and purified by sublimation at reduced pressures (ca. 10^{-2} Torr). The adsorption of (FeTMPP)₂O on the carbon surface was effected from dichloromethane solutions as described in a previous communication.⁵ The electrochemical properties of the highly dispersed material were examined by mixing the dry (FeTMPP)₂O/BP with an aqueous Teflon emulsion which serves as an inert binding agent, until the material acquired some degree of elasticity. Larger and better defined voltammetric peaks were always observed by keeping the mixtures moist (adding distilled water if necessary) during preparation and storage.

For the electrochemical measurements, a small amount of Teflon-bonded (FeTMPP)₂O/BP was applied onto the surface of a slightly recessed Tacussel solid carbon disk electrode (ca. 1-mm diameter) used for rotating disk experiments. Voltammetric measurements were performed in six different aqueous electrolytes spanning a pH range of about 12 units. The XANES spectra for the oxidized and reduced forms of the adsorbed macrocycle, however, were found to be essentially independent of the pH. The results presented in this work have been (rather arbitrarily) restricted to those obtained in experiments conducted in 0.1 M NaOH. For these measurements a gold foil was used as a counter electrode, a saturated calomel electrode as a reference. The electrochemical data were acquired with a Pine RDE-4 potentiostat/Yokowaga XY recorder system.

Iron K-edge XANES spectra were acquired at the National Synchrotron Light Source at Brookhaven National Laboratory (Line X-10C). All experiments were conducted in the fluorescence mode with a cell shown schematically in Figure 1, using a Mn filter interposed between the electrode and a pin-diode detector. A standard ion chamber with flowing dinitrogen was used to measure the incident X-ray intensity. The electrode consisted of a piece of pyrolytic graphite (2 mm × 2 mm × 15 mm) cast in Kel-F attached to a Teflon stem that enabled both rotation and translation along an axis perpendicular to the cell window. With this arrangement the entire X-ray beam could be focused onto the electrode surface. With 0.3-mm slits, the effective spectral resolution (i.e., the convolution of the total energy bandwidth of the Si(111) monochromator and the Fe-K-edge core-hole line width) was estimated

(1) For a collection of monographs in the area of in situ applications to spectroscopic techniques to the study of electrode–electrolyte interfaces, see: *Spectroelectrochemistry: Theory and Practice*; Gale, R., Ed.; Plenum Press: New York, 1988.

(2) Sharpe, L. R.; Heineman, W. R.; Elder, R. C. *Chem. Rev.* **1990**, *90*, 705.

(3) Melroy, O.; Toney, M. F.; Borges, G. L.; Samant, M. G.; Kortright, J. B.; Ross, P. N.; Blum, L. *Phys. Rev.* **1988**, *38*, 10962.

(4) Albarelli, M. J.; White, J. H.; Bommarito, G. M.; McMillan, M.; Abruna, H. D. *J. Electroanal. Chem.* **1988**, *248*, 77.

(5) Fierro, C. A.; Mohan, M.; Scherson, D. A. *Langmuir* **1990**, *6*, 1338.

(6) Torrens, M. A.; Straub, D. K.; Epstein, L. M. *J. Am. Chem. Soc.* **1972**, *94*, 4160.

[†] Case Western Reserve University.

[‡] BP Research.

[§] Lawrence Berkeley Laboratory.

[⊥] Stanford Synchrotron Radiation Laboratory.

^{*} National Institute of Standards and Technology.

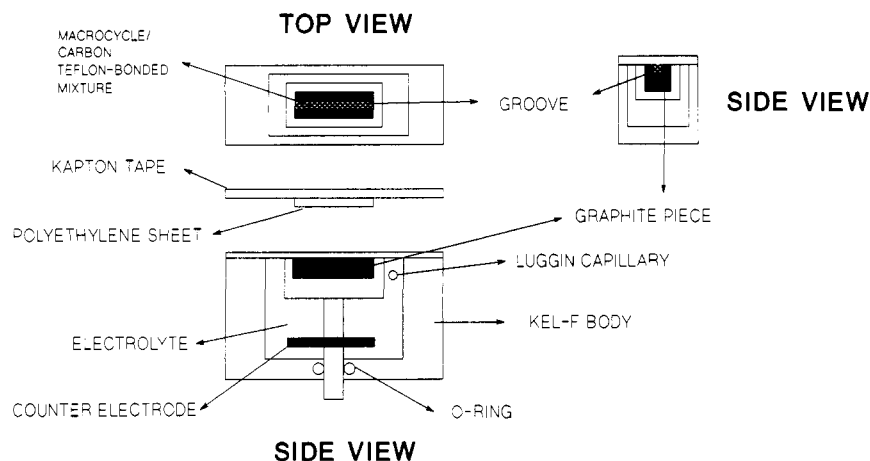


Figure 1. Schematic diagram of the electrochemical cell used for the in situ XANES measurements.

to be 2.0 eV at 7110 eV. Harmonic rejection was accomplished with a post-monochromator mirror.⁷ XANES data were obtained with a step size of 0.2 eV/point; normalization and differentiation were performed as described elsewhere.⁸ The energy calibration of each data set was maintained by use of an iron foil reference. The energy of the first inflection point in the first differential XANES for the iron foil was set to 7110.0 eV.

The Teflon/(FeTMPP)₂O/BP carbon paste was applied onto a thin, shallow groove carved along the long axis of the graphite piece. Immediately after the cell was assembled and the electrolyte was deaerated, a series of voltammetry curves were recorded with the electrode well removed from the window until features associated with the redox process could be clearly identified. During data collection, the electrode was pressed firmly against the thin polyethylene sheet (10–13 μm) attached to the back side of the Kapton tape window to avoid contact of the carbon with the adhesive backing, while passing dinitrogen continually through the bulk solution. After the initial spectra were acquired, the potential was scanned to the desired value at very small rates to avoid large capacitive (and pseudocapacitive) currents without disturbing the overall geometry. Despite the large distortions associated with the highly non-uniform current distribution, due primarily to IR drop, clear voltammetric peaks could be observed in every instance provided the potential excursion was sufficiently wide. Iron XANES spectra were recorded with the (FeTMPP)₂O in the fully oxidized and fully reduced state and, in some cases, with the electrode polarized at the redox peak potential (as determined from the undistorted voltammogram) at which both species were present in equal amounts. At least 3 min were found to be necessary upon changing the redox state of the macrocycle for the current to drop to a very small value (<1 μA).

Results

Electrochemical Aspects. The cyclic voltammetry of (FeTMPP)₂O/BP in 0.1 M NaOH, shown in Figure 2, was found to display a characteristic redox peak centered at about -0.72 V vs SCE.⁵ Although there exists some uncertainty regarding the precise amount of (total) material used in each of the experiments (on the order of a few milligrams), the integration of the voltammetric peaks appears to account for only a fraction of the amount of macrocycle present on the surface. Such seeming discrepancy is most likely caused by the formation of very small diameter, highly convoluted pores, across which ionic transport would be largely hindered. This implies that the time required for a full oxidation state conversion may be longer than that involved in the cyclic voltammetry measurements. Nevertheless, based purely on geometric arguments, assuming that the projected area of the dimer is 390 Å² and that all the carbon surface is available for adsorption, the coverage of the 40% w/w (FeTMPP)₂O is about 0.41. Some evidence that the fraction of active material is independent of the coverage was obtained by analyzing voltammetry curves for (FeTMPP)₂O/BP mixtures

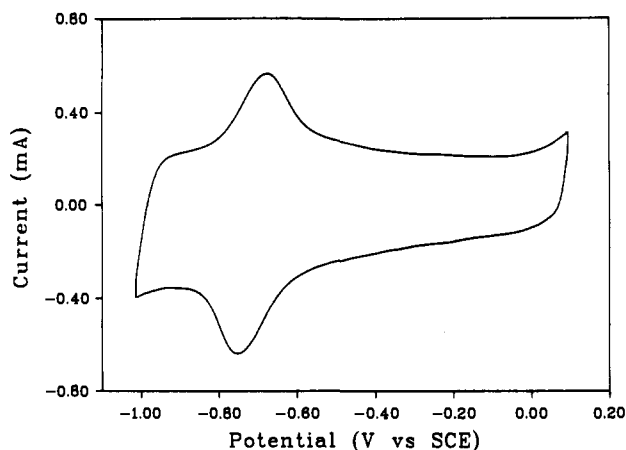


Figure 2. Cyclic voltammetry of 40% w/w (FeTMPP)₂O/BP in 0.1 M NaOH aqueous solution: scan rate, 5 mV·s⁻¹.

containing different macrocycle-to-carbon ratios. As determined from these data, plots of the charge under the redox peak normalized by the capacitive current measured at a potential away from the redox feature versus the fraction of macrocycle in the mixture were found to be linear in the range between 4 and 40% (FeTMPP)₂O. This test may be regarded as rather crude, however, as the capacitive current away from the redox peak would be proportional to the amount of carbon in the sample if and only if the interfacial capacity of the latter is not influenced by the presence of the adsorbate. As the in situ XANES measurements indicate, however (vide infra), a very large fraction of the adsorbed molecules is electrochemically active.

Voltammetric measurements as a function of pH were found to yield similar curves to those reported by Shigehara and Anson for coatings of FeTPPCl on ordinary pyrolytic graphite electrodes.⁹ In accordance with these authors, the otherwise clearly identifiable redox peaks observed under strongly acidic and strongly basic conditions became broad and ill-defined at close to neutral pH values.

It is important to note that at potentials more negative than those associated with the redox peaks, the (FeTMPP)₂O-mediated reduction of dioxygen occurs under diffusion control to generate water (as opposed to peroxide) as the product.¹⁰ Therefore, traces of dioxygen present in the electrolyte due to inefficient purging or to diffusion through the Kapton/polyethylene would be rapidly reduced to water rendering the macrocycle in the reduced state.

XANES Data. The in situ iron K-edge X-ray absorption spectrum of 40% (FeTMPP)₂O/BP in 0.1 M NaOH in the oxidized state (curve B, Figure 3) is different from that of the parent macrocycle in crystalline form (curve A, Figure 3). The first

(7) Sansone, M.; Via, G.; George, G.; Meitzner, G.; Hewitt, R.; Marsch, J. In *X-Ray Absorption Fine Structure*; Hasnain, S. S., Ed.; Ellis Horwood: London, 1991; p 656.

(8) (a) Antonio, M. R.; Brazdil, J. F.; Glaeser, L. C.; Mehicic, M.; Teller, R. G. *J. Phys. Chem.* **1988**, *92*, 2338. (b) Antonio, M. R.; Teller, R. G.; Sandstrom, D. R.; Mehicic, M.; Brazdil, J. F. *J. Phys. Chem.* **1990**, *92*, 2939.

(9) Shigehara, R.; Anson, F. C. *J. Phys. Chem.* **1982**, *86*, 2776.

(10) Tanaka, A. A. Ph. D. Thesis, Case Western Reserve University, 1987.

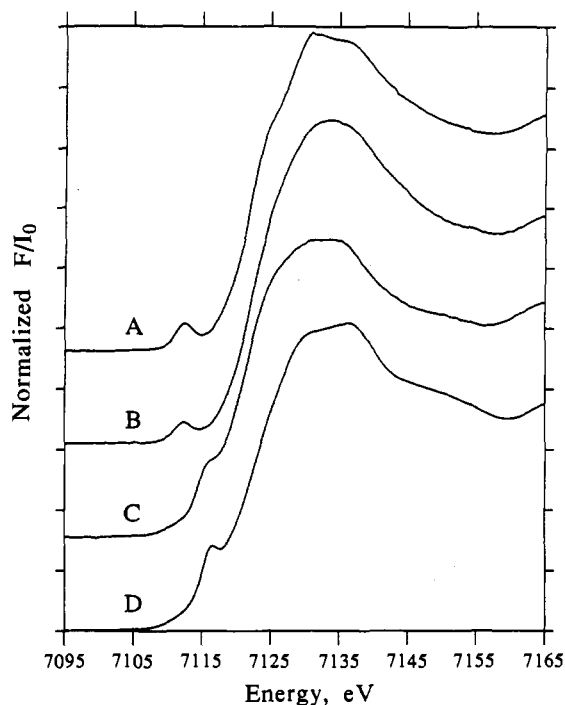


Figure 3. Normalized iron K-edge fluorescence XANES data: (A) microcrystalline $(\text{FeTMPP})_2\text{O}$ powder with five-coordinate μ -oxo bridging ligation of Fe^{3+} atoms, (B) 40% $(\text{FeTMPP})_2\text{O}/\text{BP}$ in 0.1 M NaOH in the original oxidized state, -0.43 V vs SCE, (C) 40% $(\text{FeTMPP})_2\text{O}/\text{BP}$ in 0.1 M NaOH in the reduced state, -0.90 V vs SCE, and (D) microcrystalline (phthalocyaninato)iron(II) powder with four-coordinate, square-planar Fe-N ligation of Fe^{2+} , i.e., no axial ligands. The vertical scale is offset for clarity.

differential XANES of the latter, however, shown in curve A, Figure 4, is similar to that of the closely related crystalline macrocycle (μ -oxo)bis[iron *meso*-tetrakis(phenyl)porphyrin], $(\text{FeTPP})_2\text{O}$, reported by other workers.¹¹ The pre-edge peaks at 7112.5 and 7112.4 eV for crystalline $(\text{FeTMPP})_2\text{O}$ and $(\text{FeTMPP})_2\text{O}/\text{BP}$, respectively, are sensitive indicators of the site symmetry about iron. They are due to electronic transitions from the iron 1s orbital to an empty molecular orbital with iron 3d character.¹² The normalized intensities of the 1s \rightarrow 3d peaks for the crystalline (0.115) and adsorbed (0.093) $(\text{FeTMPP})_2\text{O}$ on BP are consistent with those known for five-coordinate μ -oxo-bridged Fe^{3+} macrocycles.¹³⁻¹⁵ Inspection of the XANES (Figure 3) and first differential XANES (Figure 4) reveals a diminution of the pre-edge peak and an alteration of the edge peak of crystalline $(\text{FeTMPP})_2\text{O}$ upon adsorption of the macrocycle on the surface and subsequent exposure to the electrolyte. These effects are most obvious in the first differential XANES (curves A and B, Figure 4) upon comparison of the widths and shapes of the peaks at ca. 7122 eV and the intensities of the peaks at ca. 7111.0 eV, which are the edge and pre-edge peak inflection points, respectively. Furthermore, the inflection points at ca. 7128 and 7135 eV in the first differential XANES for crystalline $(\text{FeTMPP})_2\text{O}$ are not resolved in those data for adsorbed $(\text{FeTMPP})_2\text{O}$ (Figure 4). These differences may be ascribed to a molecular relaxation induced by the removal of the macrocycle from its original crystal lattice, a process that could generate a multiplicity of closely related iron environments ($\cdots\text{Fe}^{3+}-\text{O}-$

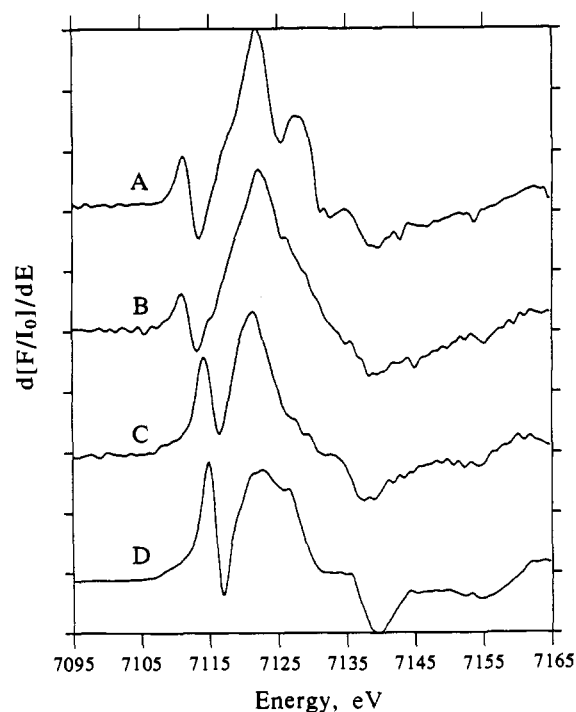


Figure 4. First differential iron XANES of the data shown in Figure 3. The order of the curves is the same as that identified in the caption to Figure 3. The vertical scale is offset for clarity.

$\text{Fe}^{3+}\cdots$) and thus lead to alterations of the XANES of the type found in this study. The first of these effects may explain, at least partially, the marked losses in the recoilless fraction observed for the same material in similar environments for which no ^{57}Fe Mossbauer effect spectra could be obtained at room temperature even in the absence of electrolyte.⁵

Pronounced changes in the iron XANES were observed (curve C, Figure 3) upon polarizing the electrode at a potential negative enough for the adsorbed macrocycle to undergo complete reduction. Most prominent is the disappearance of the pre-edge peak at 7112.4 eV for the oxidized macrocycle and the shift in the onset of the absorption edge with the appearance of a new, incompletely resolved pre-edge peak at ca. 7116 eV. The first differential XANES (curve C, Figure 4) reveals two strong peaks at 7114.3 and 7121.5 eV, corresponding to the pre-edge and edge inflection points, respectively. The presence of this new pre-edge peak for the fully reduced, supported macrocycle is indicative of a four-coordinate, square-planar environment about iron. Such pre-edge peaks are characteristic of four-coordinate square-planar complexes of Fe^{2+} ,¹¹ such as for iron *meso*-tetrakis(phenyl)porphyrin as well as for those of Cu^{2+} ¹⁶ and Ni^{2+} .¹⁷ By analogy with previous assignments,^{16,17} the pre-edge peak observed in Figure 3 for the reduced, adsorbed macrocycle is due to an electronic transition from the iron 1s orbital to an empty $4p_z$ orbital.

The XANES and first differential XANES for iron(2+) phthalocyanine (with 4-fold, square-planar Fe-N coordination and no axial ligation) are also shown in curve D, Figures 3 and 4, respectively. Note the well-resolved pre-edge peak at 7116.6 eV with an inflection point energy of 7115.0 eV. Comparison of these data with those for the reduced, adsorbed porphyrin (in the same figures) reveals an important similarity, namely, the presence of pre-edge peaks of nearly equal magnitude at about 7116 eV,

(11) Penner-Hahn, J. E.; McMurry, T. J.; Renner, M.; Latos-Grazynsky, L.; Smith-Eble, K.; Davis, I. M.; Balch, A. L.; Groves, J. T.; Dawson, J. H.; Hodgson, K. O. *J. Biol. Chem.* **1983**, *258*, 12761.

(12) Penner-Hahn, J. E.; Hodgson, K. O. In *Iron Porphyrins*, Part III, Lever, A. B. P.; Gray, H. B., Eds.; VCH Publishers: New York, 1989; pp 236-304.

(13) Co, M. S. *SSRL Report*, 84/02, 1983; pp 145-193.

(14) Roe, A. L.; Schneider, D. J.; Que, L. Jr. *J. Am. Chem. Soc.* **1984**, *106*, 1676.

(15) Kauzlarich, S. M.; Teo, B. K.; Zirino, T.; Burman, S.; Davis, J. C.; Averill, B. A. *Inorg. Chem.* **1986**, *25*, 2781.

(16) (a) Smith, T. A.; Penner-Hahn, J. E.; Berding, M. A.; Doniach, S.; Hodgson, K. O. *J. Am. Chem. Soc.* **1985**, *107*, 5945. (b) Smith, T. A.; Penner-Hahn, J. E.; Hodgson, K. O.; Berding, M. A.; Doniach, S. *Springer Proc. Phys.* **1984**, *2*, 58.

(17) (a) Eidsness, M. K.; Sullivan, R. J.; Schwartz, J. R.; Hartzell, P. L.; Wolfe, R. S.; Flank, A. M.; Cramer, S. P.; Scott, R. A. *J. Am. Chem. Soc.* **1986**, *108*, 3120. (b) Eidsness, M. K.; Sullivan, R. J.; Cramer, S. P.; Scott, R. A. In *Bioinorganic Chemistry of Nickel*; Lancaster, J. R., Ed.; VCH Publishers: Deerfield Beach, FL, 1987; pp 73-91.

which are characteristic of Fe^{2+} four-coordinate square-planar geometry. The apparent resolution of the pre-edge peak (due to a $1s \rightarrow 4p_z$ electronic transition) for the reduced, adsorbed macrocycle is clearly less than that for either crystalline FePc (recorded under the same experimental conditions) or iron *meso*-tetrakis(phenyl)porphyrin.¹² There are at least two plausible explanations for this effect: (i) a multiplicity of closely related iron environments (all with 4-fold square-planar coordination) due to structural distortions of the TMPP framework upon adsorption and reduction of the parent macrocycle and (ii) a heterogeneity of coordination, such that the principal fraction of iron in the reduced, adsorbed macrocycle is four-coordinate square-planar and a small fraction is five- or six-coordinate with distant axial ligands. The latter would be the case if, for example, some of the adsorbed material is not in either electronic or electrolytic contact with the rest of the system. Nevertheless, upon polarizing the electrode at a potential positive enough to reoxidize the adsorbed FeTMPP , the XANES data obtained were essentially identical to those shown in curve B, Figure 3, for the fully oxidized $(\text{FeTMPP})_2\text{O}/\text{BP}$ complex. This indicates that, to the level of sensitivity of the measurements, the redox process is reversible. This may be regarded as rather surprising in view of the large structural rearrangements associated with the reformation of the μ -oxo framework.

Experiments conducted in solutions of 0.05 M H_2SO_4 (pH = 1) and 0.0015 M NaOH , 0.05 M H_3BO_3 , and 0.05 M Na_2SO_4 (pH = 8.7), for which XANES were recorded at intermediate

potentials (see supplementary material), were characterized by the presence of at least two isosbestic points, as would be expected for the interconversion of one species into the other.

Conclusions

The in situ iron XANES described herein provides conclusive evidence, for the first time, that the coordination about Fe^{2+} in the supported, fully reduced macrocycle is remarkably different from that about Fe^{3+} in the corresponding fully oxidized macrocycle. It is thus concluded from the iron K-edge XANES results that $(\text{FeTMPP})_2\text{O}$ in the adsorbed state retains its μ -oxo character and undergoes a two-electron reduction to yield predominantly axially uncoordinated FeTMPP . This assignment is in agreement with earlier in situ ^{57}Fe Mossbauer effect measurements on the same system in which the isomer shift and quadrupole splitting of the reduced species observed at about 250 K were consistent with those of a ferrous porphyrin species.⁵

Acknowledgment. This work was supported by the Gas Research Institute. Research was carried out (in part) at the National Synchrotron Light Source, Brookhaven National Laboratory, which is supported by the U.S. Department of Energy, Division of Materials Sciences and Division of Chemical Sciences (DOE Contract No. DE-AC02-76CH0016).

Supplementary Material Available: Plot of F/I_0 vs energy for normalized iron K-edge fluorescence XANES data (1 page). Ordering information is given on any current masthead page.

Chemical and Spectroscopic Studies of the Mixed-Valent Derivatives of the Non-Heme Iron Protein Hemerythrin

James M. McCormick, Richard C. Reem, and Edward I. Solomon*

Contribution from the Department of Chemistry, Stanford University, Stanford, California 94305. Received August 20, 1990

Abstract: The electronic transitions of the mixed-valent $[\text{Fe(II)}, \text{Fe(III)}]$ form of the binuclear non-heme iron protein hemerythrin are assigned using absorbance, circular dichroism, and low-temperature magnetic circular dichroism (MCD) spectroscopies. $^{1/2}\text{Met}_r$ (prepared by reduction of met) and the ligand bound forms are found to have both irons in octahedral ligand geometries, while for $^{1/2}\text{met}_o$ (prepared by oxidation of deoxy) the Fe^{2+} is five-coordinate and the Fe^{3+} is six-coordinate. Variable-temperature MCD and EPR spectroscopies are used to probe the ground-state magnetic properties; all $^{1/2}\text{met}$ forms are found to have $J \approx -8 \text{ cm}^{-1}$, consistent with an endogenous bridging OH^- . $^{1/2}\text{Met}_r$ and $^{1/2}\text{met}_o$ are found to be in a pH-dependent equilibrium, reflecting binding of OH^- as an exogenous ligand. The differences in geometric and electronic structure between $^{1/2}\text{met}_r$ and $^{1/2}\text{met}_o$ are related to the redox reactivity of this active site.

Introduction

A coupled binuclear non-heme iron active site occurs in a variety of different enzymes and proteins whose function often involves reaction with dioxygen. Members of this class of proteins (and their dioxygen reactivities) include the following: hemerythrin (Hr, oxygen transport and storage),¹ ribonucleotide diphosphate reductase (RDPR, formation of a catalytically active tyrosine radical),² methane monooxygenase (MMO, activation of dioxygen

for insertion into carbon-hydrogen bonds),³ the purple acid phosphatases (PAP, inactivated by dioxygen in the presence of phosphate),⁴ and rubrerythrin (Rb, unknown).⁵ The binuclear iron site can exist in three oxidation states: met $[\text{Fe(III)}, \text{Fe(III)}]$, $^{1/2}\text{met}$ (or semimet) $[\text{Fe(II)}, \text{Fe(III)}]$, and deoxy (or fully reduced) $[\text{Fe(II)}, \text{Fe(II)}]$. All three oxidation states can be obtained for

(1) (a) Wilkins, P. C.; Wilkins, R. G. *Coord. Chem. Rev.* **1987**, *79*, 195-214. (b) Klotz, I. M.; Kurtz, D. M., Jr. *Acc. Chem. Res.* **1984**, *17*, 16-22.
(2) (a) Stubbe, J. J. *Biol. Chem.* **1990**, *265*, 5329-5332. (b) Sjöberg, B.-M.; Gråslund, A. Ribonucleotide Reductase. In *Advances in Inorganic Biochemistry Vol. 5*; Thell, E. C., Elchorn, G. L., Marzilli, L. G., Eds.; Elsevier: 1983; pp 87-110. (c) Reichard, P.; Ehrenberg, A. *Science* **1983**, *221*, 514-519.

(3) (a) Dalton, H. Oxidation of Hydrocarbons by Methane Monooxygenase from a Variety of Microbes. In *Advances in Applied Microbiology*; Umbreit, W. W., Ed.; Academic Press: 1980; pp 71-87. (b) Fox, B. G.; Froland, W. A.; Dege, J. B.; Lipscomb, J. D. *J. Biol. Chem.* **1989**, *264*, 10023-10033.

(4) Doi, K.; Antanaitis, B. C.; Aisen, P. The Binuclear Iron Centers of Uteroferrin and the Purple Acid Phosphatases. In *Structure and Bonding 70*; Springer-Verlag: Berlin, 1988; pp 1-26.

(5) LeGall, B. G.; Prickril, B. C.; Moura, I.; Xavier, A. V. *Biochemistry* **1988**, *27*, 1636-1642.